Int. J. Electrochem. Sci., 6 **(2011)** 3333 - 3343

International Journal of
ELECTROCHEMICAL
SCIENCE
www.electrochemsci.org

Enhancement of Dye-Sensitized Solar Cells by using Graphene-TiO_2 Composites as Photoelectrochemical Working Electrode

Tsung-Hsuan Tsai, Shr-Chiang Chiou, Shen-Ming Chen[*]

Electroanalysis and Bioelectrochemistry Lab, Department of Chemical Engineering and Biotechnology, National Taipei University of Technology, No.1, Section 3, Chung-Hsiao East Road, Taipei 106, Taiwan (ROC).
[*]E-mail: smchen78@ms15.hinet.net

Received: 17 June 2011 / *Accepted:* 16 July 2011 / *Published:* 1 August 2011

Composite films of graphene-content TiO_2 were deposited on indium tin oxide (ITO) substrates by spin coating at room temperature and applied as working electrodes of dye-sensitized solar cells (DSSCs). Field emission scanning electron microscope (FE-SEM) and atomic force microscopes (AFM) measurements show that a uniform graphene is formed around the TiO_2 particles and mapping of the porous TiO_2 layer that the graphene distribution is uniform throughout the layer. The amount of dye absorption is increased with increase in the content of graphene and cyclic voltammetry (CV) measurement show a gradual increase in the anodic current. With an optimum content of graphene (1wt %) involve in TiO_2 film, a 15% improvement in the cell efficiency (from 5.98% to 6.86%) is achieved.

Keywords: Dye-sensitized solar cells, Graphene, Cyclic voltammetry, N719 dye, Carbon materials, Photoelectrochemistry

1. INTRODUCTION

Dye sensitized solar cells (DSSCs) have aroused much attention as a cheap and next generation solar cell. It is well known that a typical dye-sensitized solar cell (DSSC) consists of porous TiO_2 film, dye molecules which are sensitive to sunlight, and an organic liquid electrolyte, essentially containing iodide and triiodide ions as a redox couple [1, 2]. These three layers are sandwiched together between two conducting glasses, one covered with a thin layer of TiO_2 and the other with a platinum layer. DSSCs show considerable potential as a relatively low cost alternative to silicon based solar cells. These cells were developed by Gratzel and co-workers in 1991 [3] and there is currently a considerable focus on enhancing their light conversion efficiency and stability [4–11]. In the case of conventional

DSSCs, dye sensitization involves solely the semiconductor anode made of n-type TiO_2 nanoparticles. The counter electrode is generally a metallic cathode with no photoelectrochemical activity [3–11]. The efficiency, however of p-type metal oxides is still very low, which limits their effectiveness in tandem DSSCs [12]. One method of improving this efficiency would be the preparation of p-type metal electrodes with a surface exhibiting high porosity without sacrificing the mechanical stability of the resulting coatings. This surface morphology ensures higher light absorption by the monolayer of adsorbed dye, while keeping an intimate contact between the p-type material and the dye molecules. This in turn reduces the inner resistance and hence improving the charge injection efficiency.

Carbon materials have attracted a great deal of interests for both scientific fundamentals and potential applications in various new optoelectronic devices [13], such as graphite [14], carbon black [15], mesoporous carbon [16], carbon nanotube (CNT) [17–19], and graphene [20–22]. Among various carbon materials, the graphene is a single-layer structure of two-dimensional graphite. Monolayer graphene is highly transparent (only one atom thick) and absorbs only 2.3% of incident white light [23]. Similar to CNTs, graphene is highly conductive and extremely strong. The energy gap of graphene can be tuned and scales inversely with the width [24]. These remarkable electronic properties qualify graphene for applications in future optoelectronic devices.

In this paper, we describe a spin coating method to prepare different graphene-content TiO_2 composite film on ITO electrode substrates. The amount of graphene in composite film varied from 0.00 wt% to 1 wt%. It was observed that the introduction of graphene into photoanode successfully used as a working electrode and significantly influenced the performance of DSSCs. The photovoltaic performances of the devices were analyzed.

2. EXPERIMENTAL

2.1 Materials and chemicals

P25 TiO_2 powder, N719 dye, 4-t-butylpyridine (TBP), Triton X-100 solution and PEG 20000 were purchased from Sigma-Aldrich (USA). Indium tin oxide (ITO) (7 $\Omega \cdot cm^{-2}$) was purchased from Merck Display Technologies (MDT) Ltd (Taiwan). Lithium iodide (LiI, analytical grade), and iodine (I_2, analytical grade) were obtained from Wako (Japan). 60 μm thick surlyn films were purchased from Solaronix S.A., Aubonne, (Switzerland). Double distilled deionized water (DDDW) was used to prepare all the solutions.

2.2. Apparatus

All electrochemical experiments were performed using a CHI 750a potentiostat (CH Instruments, USA). Electrochemical impedance studies (EIS) were performed using a ZAHNER impedance analyzer (Germany). UV–visible spectra were obtained using Hitachi U-3300 spectrophotometer (Japan). The atomic force microscope (AFM) images were recorded using a

multimode scanning probe microscope (Being Nano-Instruments CSPM-4000, China). Field emission scanning electron microscope (FE-SEM) images were recorded using a HITACHI S-4700 (Japan).

2.3 Preparation of graphene-content TiO_2 films on ITO substrates

Nano graphene-content TiO_2 films on ITO substrates were deposited as follows, 9 g P-25 TiO_2 powder with different weight of graphene, 0.1 ml Triton X-100, 1g PEG 20000 and 18 ml DDDW were mixed well in a dried agate mortar for one hour. The final mixture was stirred for an additional 2 days to obtain the desired TiO_2 paste. The above obtained TiO_2 paste solution was spin-coated on an ITO glass substrate at 1000 rpm for 10 s and 2000 rpm for 30 s. The formed film was annealed at 450 °C for 1 hour in atmosphere. These graphene-content (0wt %~10wt %) TiO_2 film coated on ITO were dried at room temperature for several minutes and then heated at 150 °C for 30 min, on a hotplate, in the atmospheric conditions. After heating at 150 °C and cooling to room temperature, the graphene-content (0wt %~10wt %) TiO_2 electrodes were immersed in a 5×10^{-4} M solution of N719 in acetonitrile and tert-butyl alcohol for 1 day. The thus prepared graphene-content (0wt %~10wt %) TiO_2 electrodes were coupled with a platinum-sputtered conducting glass electrode (Pt/ITO). The electrodes were separated by a 60 □m thick surlyn film and sealed together by heating. A thin layer of electrolyte was introduced into the inter electrode space. The electrolyte contains 0.1 M LiI, 0.05 M I_2, and 0.5 M 4-tertbutylpyridine (TBP) in dehydrated acetonitrile.

3. RESULTS AND DISCUSSION

3.1 Surface morphology of grapheme-content TiO_2 electrodes

The surface morphology of graphene-content TiO_2 film has been examined using AFM and SEM. Here the AFM studies could furnish the comprehensive information about the surface morphology of graphene-content TiO_2 coated on the ITO surface. Fig. 1A and 1B show the FE-SEM micrograph of 0wt % graphene-content TiO_2 and 10wt % graphene-content TiO_2 films coated on the ITO surface. Fig. 1C and 1D show the AFM images of 0wt % graphene-content TiO_2 and 10wt % graphene-content TiO_2 films coated on the ITO surface and examined by using the tapping mode. Fig. 1E and 1F shows the cross-sectional and granularity normal distribution chart of 0wt % graphene-content TiO_2 and 10wt % graphene-content TiO_2 films coated on the ITO surface. The AFM parameters have been evaluated for 2000 × 1900 nm surface area. The nano bare TiO_2 particles and nano 10wt % graphene-content TiO_2 particles in the obvious manner were found to 43.3 nm and 17.2 nm. Average height of bare TiO_2 and 10wt % graphene-content TiO_2 films were found as 15.4 nm and 13.3 nm. The above AFM and FE-SEM results clearly illustrate the surface nature of bare TiO_2 and 10wt % graphene-content TiO_2 films coated on the ITO surface. By AFM roughness analysis, roughness factors obtained are increased as increasing the content of graphene in TiO_2 film with the maximum value in 1wt % graphene-content TiO_2 as listed in Table 1. The highest roughness factor of

1wt % graphene-content TiO_2 film may be attributed to the decreased crystallinity in comparison with 0wt %, 0.01wt %, 0.1wt % and 10wt % graphene-content TiO_2 [25-27].

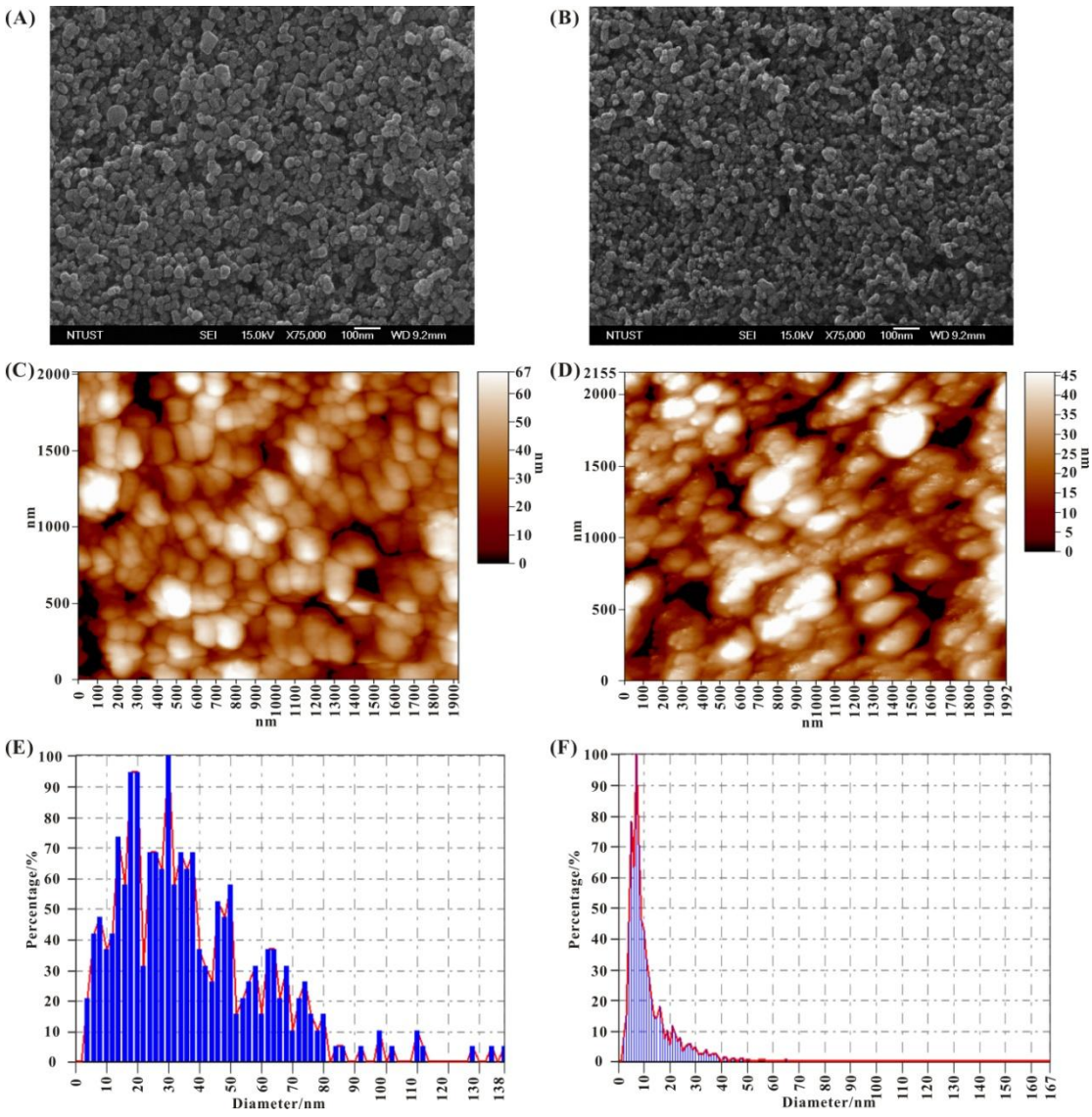

Figure 1. SEM image of TiO_2 film containing (A) 0wt % and (B) 1wt % graphene, tapping mode AFM image of TiO_2 film containing (C) 0wt % and (D) 1wt % graphene and granularity normal distribution chart for the TiO_2 film containing (E) 0wt % and (F) 1wt % graphene.

Table 1. Physicochemical properties of DSSCs based on various graphene-content TiO_2 films.

Sample number	Graphene content (%)	NP size (nm)	Roughness (nm)	R_{ct1} (Ω)	R_{ct2} (Ω)
1	0	43.28	10.2	9.09	13.37
2	0.01	38.13	10.3	10.52	19.92
3	0.1	31.95	12.3	10.92	25.01
4	1	25.52	21.1	8.25	17.41
5	10	17.23	14.5	8.70	31.11

3.2 Electrocatalytic activity at graphene-content TiO_2 photo anode electrode

The performances of the DSSCs with photo anodes embedded with different contents of graphene in TiO_2 film were examined.

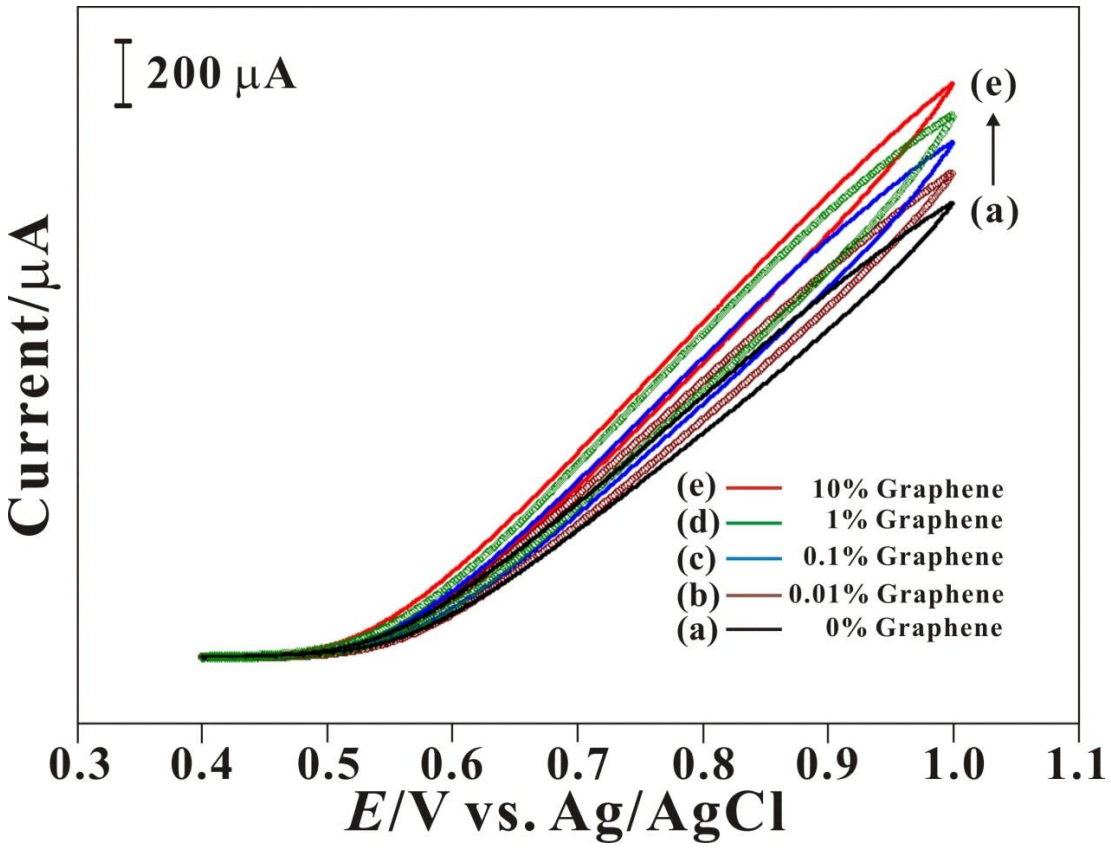

Figure 2. CVs of TiO_2 film containing 0wt %, 0.01wt %, 0.1wt %, 1wt % and 10wt % graphene in an acetonitrile solution with 0.01M LiI, 0.001M I_2 and 0.1M $LiClO_4$ containing 5 mM N719 dye, initial E = 0.4 V, high E = 1.0 V, low E = 0.4 V, scan rate = 50mVs^{-1}.

The results show an improvement in dye absorption with increase in the contents of graphene, as shown in Fig. 2. This is mainly due to that the high specific surface area and many chemical defects of ultrathin graphene sheets can disperse nanostructures with high surface area toward absorption of dye [28, 29]. Meanwhile, TiO_2 film is embedded a highly conductive matrix around graphene sheets [30]. To investigate the effects of graphene content on the performances of DSSCs, a series of working electrodes were prepared from the mixtures with different contents of graphene. As the graphene content in the mixture increased from 0wt % to 10wt %, the anodic current of cyclic voltammetry (CV) showed a gradual increase in Fig. 2. Curve a–e of Fig. 2 show that there is a gradual increase in the anodic current at TiO_2 film with different contents of graphene (0, 0.01, 0.1, 1 and 10wt %) coated on ITO electrode in an acetonitrile solution with 0.01 M LiI, 0.001 M I_2, 0.1 M $LiClO_4$ and 5×10^{-4} M N719 dye. All the above results indicate that using the graphene involved in TiO_2 film for photo anode electrode can help to enhance the electro catalytic reaction and absorption of N719 dye.

3.3 The light-scattering and dye adsorption abilities of the photo anodes

To determine the amount of dye absorbed on bare and graphene-content TiO_2 (0, 0.01, 0.1, 1 and 10wt %), the dyes were desorbed from TiO_2 photoelectrodes using 0.1 M NaOH and the absorbance of the solution was measured with a UV–vis spectroscope. The results show an improvement in dye absorption with increase in the contents of graphene, as shown in Fig. 3.

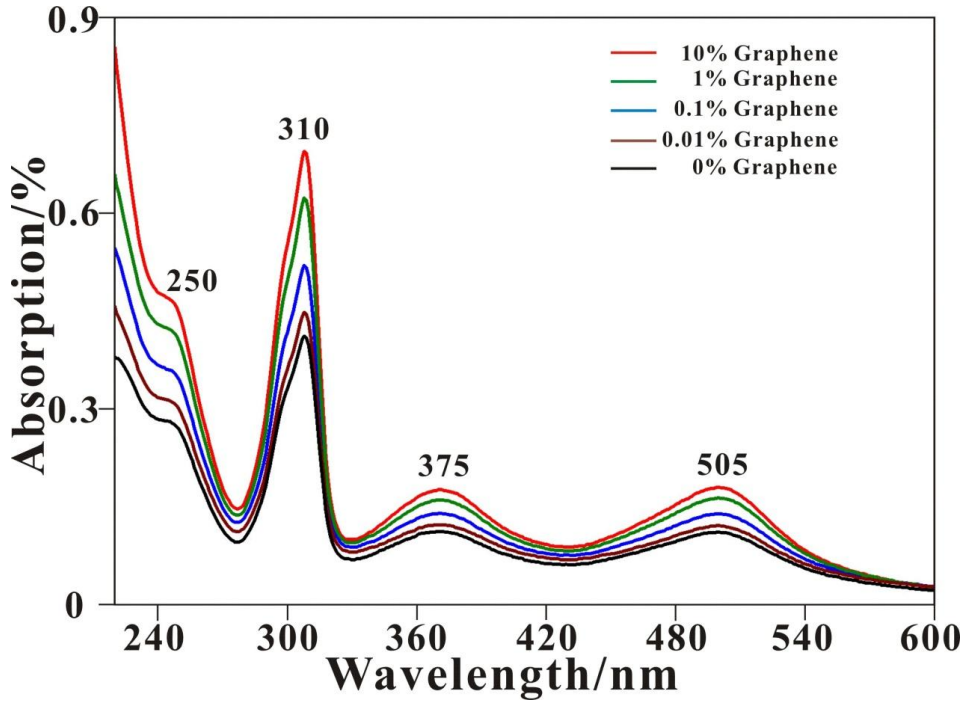

Figure 3. Typical UV-vis spectra of dye desorbed from TiO_2 film containing 0wt %, 0.01wt %, 0.1wt %, 1wt % and 10wt % graphene by using 0.1 M NaOH.

This might be grapheme can help spread the TiO_2 particles and enhance the adsorption of dye. The absorption peaks at around 310, 375 and 566 nm which were characteristic of N719 dye [31-33]. The above results showed the addition of graphene successful enhance the adsorption of N719 dye.

3.4 DSSCs photovoltaic properties

3.4.1 Photoelectric performances of DSSCs

Fig. 4 illustrates the photocurrent-voltage curves of the cells with graphene-content TiO_2 working electrodes under full sunlight of 100 mW cm^{-2} (AM 1.5) conditions, respectively. The open-circuit voltage (V_{oc}), short-circuit photocurrent density (J_{sc}), fill factor (FF) and efficiency (η) of the cells are listed in Table 2. Energy conversion efficiency of the DSSCs using the graphene-content TiO_2 composite film contained 1wt % graphene as working electrode was measured to be 6.86% and the J_{sc},

FF and V_{oc} were higher than those of the DSSCs with 0wt % graphene-content TiO_2 working electrode.

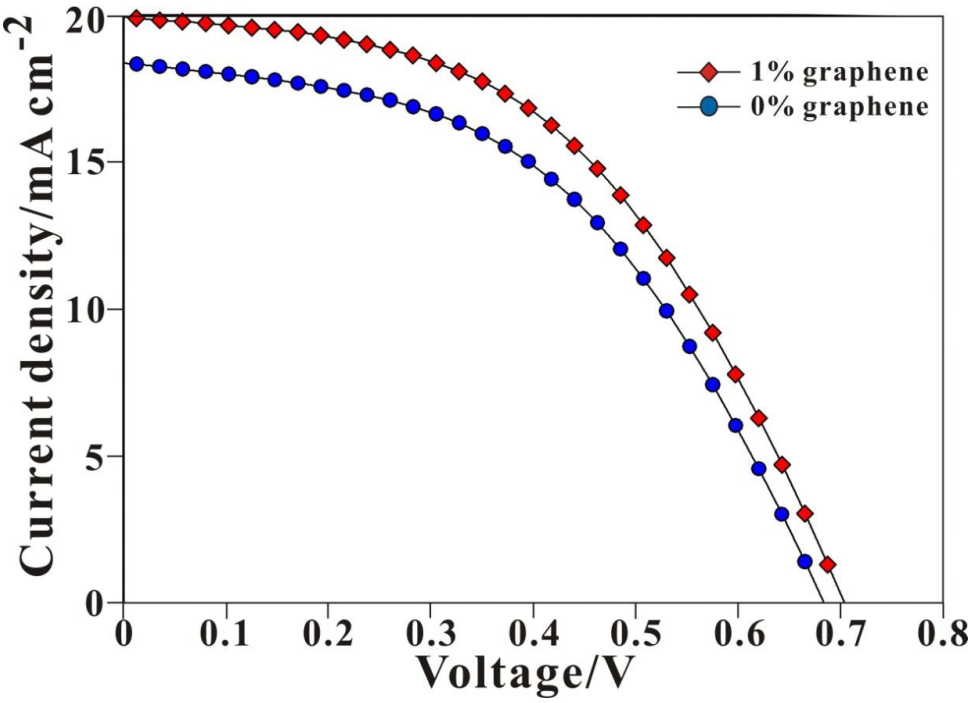

Figure 4. Current–voltage (I–V) characteristics of solar cell with TiO_2 film containing 0wt % and 1wt % graphene measured at one sun illumination (100 mW cm^{-2}, AM 1.5).

Table 2. The photovoltaic parameters of DSSCs based on various graphene-content TiO_2 films.

Sample number	Graphene content (%)	J_{sc} (mA cm^{-2})	V_{oc} (V)	FF%	η%
1	0	18.83	0.684	46.48	5.98
2	0.01	19.87	0.699	45.40	6.32
3	0.1	19.55	0.699	48.04	6.57
4	1	19.92	0.704	48.86	6.86
5	10	17.88	0.747	47.06	6.29

However, the difference contents of graphene TiO_2 and 0wt % graphene-content TiO_2 limited the performance. Compared to 0wt % graphene-content TiO_2 film, the addition of a small amount of graphene sheets effectively increased the short-circuit photocurrent densities and fill factors of the cells. This is mainly due to that the high specific surface area and many chemical defects of ultrathin graphene sheets provide them with highly dispersion of the TiO_2 particles and enhance the adsorption of dye [14, 22, 34]. To investigate the effects of graphene content on the performances of DSSCs, a series of working electrodes were prepared from the mixtures with different graphene contents. As the contents of graphene involved in TiO_2 film increased from 0wt % to 1wt %, the energy conversion

efficiency of the DSSC was increased from 5.98% to 6.86% (Table 2). However, further increasing the weight content of graphene showed little effect on the energy conversion efficiency of the cells. These results indicate that a small amount of graphene (1wt %) is sufficient for electrochemical catalyzation and can effectively improve the cell performances.

3.4.2 Optimum condition of the contents for DSSCs

When we further increased the contents of graphene involved in TiO_2 film in the range of 0, 0.01, 0.1, 1 and 10wt %, the V_{oc} values were slightly increased because of the graphene-content TiO_2 enhanced the absorption of dye, as shown in Fig. 5A.

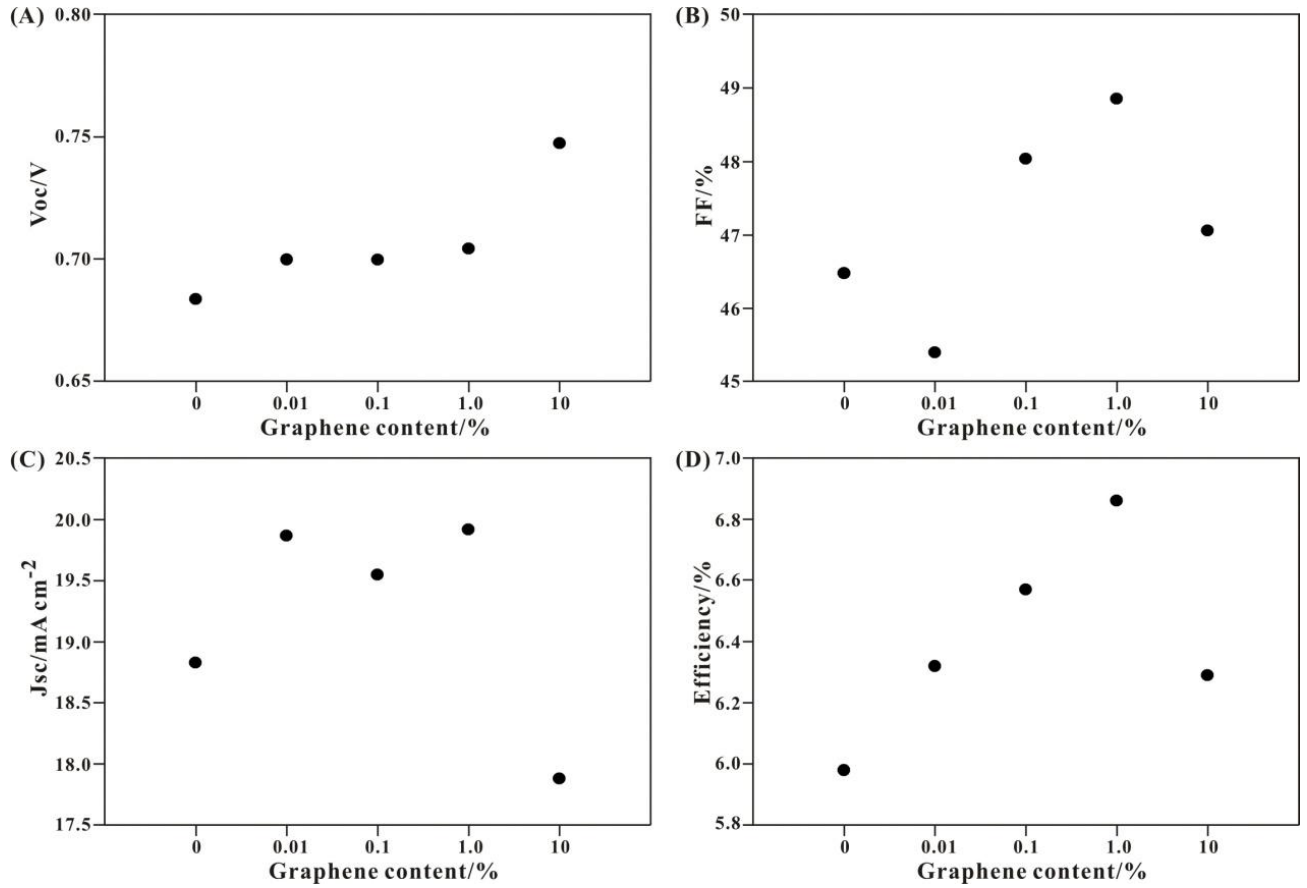

Figure 5. Standard DSSC with TiO_2 containing 0%, 0.01%, 0.1%, 1% and 10% graphene for the photocurrent density–voltage characteristics (A) V_{oc}, (B) FF%, (C) J_{sc} and (D) efficinecy%.

By the same way, these values of FF, J_{sc} and η also increased with the graphene content, until a decrease when the graphene content up to 10wt % (Fig. 5B, C and D). This might be high graphene content involved TiO_2 film increased the surface resistance of the TiO_2 electrode and with further increase in film thickness. In the case, by increasing the graphene content for the improvement of

efficiency is not substantial but the graphene involved in TiO_2 film improves the current and other cell parameters by suppressing the electron recombination.

3.4.3 AC impedance spectra of DSSCs

AC impedance spectroscopy of DSSCs revealed three semicircles that correspond to different frequency ranges [35-37].

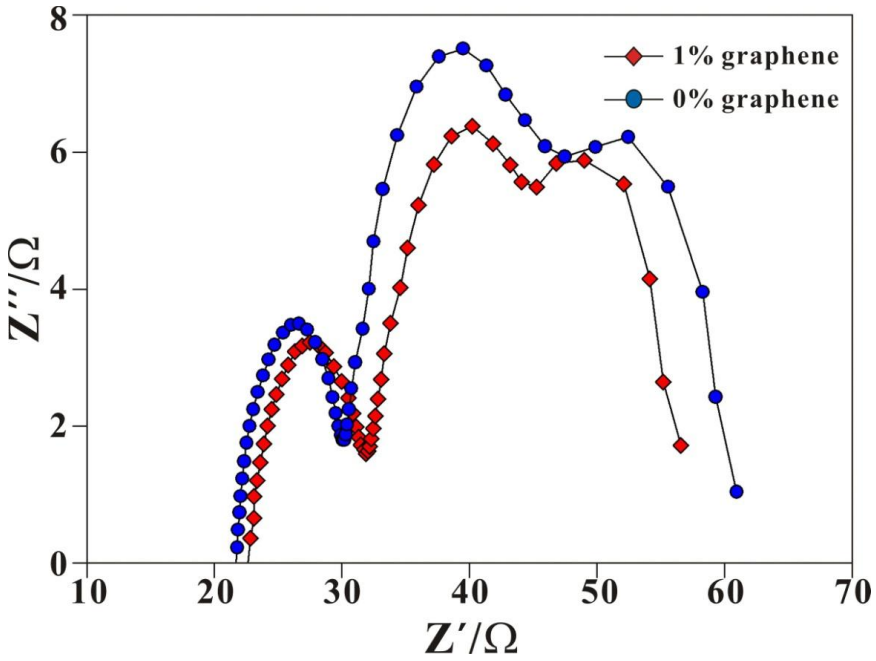

Figure 6. Impedance plot of solar cell with TiO_2 film containing 0wt % and 1wt % graphene measured at one sun illumination (100 mW cm^{-2}, AM 1.5).

The first semicircle (R_{ct1}) indicated the one in the high-frequency region, is attributed to the impedance of the charge-transfer process at the counter electrode. The second semicircle (R_{ct2}) indicated the one in the middle-frequency region, is related to the charge-transfer process at the TiO_2|dye|electrolyte interface as well as the resistance to the transport of electrons to the conduction electrode on the glass substrate. The third arc (R_{diff}) was in the low-frequency range which attributed to Nernstian diffusion in the electrolyte. Tail of the third arc becomes longer when the thickness of the electrolyte layer is increased by placing a counter electrode far from a working electrode [38, 39]. The AC impedance of the cells was measured at open-circuit voltage under full sunlight of 100 mW cm^{-2} (AM 1.5) conditions with electrochemical impedance spectroscope (EIS), as shown in Fig. 6 and Table 1. The AC impedance spectra clearly showed that the semicircles (high-frequency region range from 100 KHz to 100 Hz) for DSSCs used 1wt % graphene-content TiO_2 photo anode electrode became smaller than the DSSCs used bare TiO_2 photo anode electrode. Thus indicating a lower interfacial charge transfer resistance at the interface between 1wt % graphene-content TiO_2 photo anode electrode and electrolyte.

4. CONCLUSION

A graphene-content TiO_2 photo anode electrode by spin-coating has been demonstrated as a means of increasing the efficiency of dye-sensitized solar cells. The graphene content involved in TiO_2 film reduces the loss of electrons by suppressing their recombination, and this results in a significant increase in the short-circuit current and the overall power conversion efficiency. The improvement is also obtained from enhancement of dye absorption on the graphene-content TiO_2 film surface. It is confirmed that the optimum content of graphene involved TiO_2 film is 1 wt% for high-performance DSSCs and showed a high energy conversion efficiency of 6.86% under full sunlight of 100 mW cm^{-2} (AM 1.5) conditions.

ACKNOWLEDGMENT
This work was supported by the National Science Council of Taiwan.

References

1. L. Y. Lin, C. P. Lee, R. Vittal and K. C. Ho, *J. Power Sources*, 196 (2011) 1671.
2. Z. Wei, Y. Yao, T. Huang and A. Yu, *Int. J. Electrochem. Sci.*, 6 (2011) 1871.
3. B. O'Regan and M. Gratzel, *Nature*, 353 (1991) 737.
4. S. J. Lue, P. W. Lo, L. Y. Hung and Y. L. Tung, *J. Power Sources*, 195 (2010) 7677.
5. M. H. Lai, M. W. Lee, G. J. Wang and M. F. Tai, *Int. J. Electrochem. Sci.*, 6 (2011) 2122.
6. T. D. Nielsen, C. Cruickshank, S. Foged, J. Thorsen and F.C. Krebs, *Sol. Energy Mater. Sol. Cells*, 94 (2010) 1553.
7. H. Xu, X. Tao, D. T. Wang, Y. Z. Zheng and J. F. Chen, *Electrochim. Acta*, 55 (2010) 2280.
8. H. Tributsch, *Coord. Chem. Rev.*, 248 (2004) 1511.
9. S. Anandan, *Sol. Energy Mater. Sol. Cells*, 91 (2007) 843.
10. M. A. Green, K. Emery, Y. Hishikawa and W. Warta, *Prog. Photovoltaics Res. Appl.*, 17 (2009) 85.
11. J. L. Lan, C. C. Wan, T. C. Wei, W. C. Hsu, C. Peng, Y. H. Chang and C. M. Chen, *Int. J. Electrochem. Sci.*, 6 (2011) 1230.
12. S. Sumikura, S. Mori, S. Shimizu, H. Usami and E. Suzuki, *J. Photochem. Photobiol.*, A199 (2008) 1.
13. H. Zhu, J. Wei, K. Wang and D. Wu, *Sol. Energy Mater. Sol. Cells*, 93 (2009) 1461.
14. X. Hu, K. Huang, D. Fang and S. Liu, *Materials Science and Engineering B*, 176 (2011) 431.
15. Y. S. Park and H. K. Kim, *Current Applied Physics*, 11 (2011) 989.
16. E. Ramasamy and J. Lee, *Carbon*, 48 (2010) 3715.
17. J. Zhang, X. Li, W. Guo, T. Hreid, J. Hou, H. Su and Z. Yuan, *Electrochimica Acta*, 56 (2011) 3147.
18. C. T. Hsieh, B. H. Yang and J. Y. Lin, *Carbon*, 49 (2011) 3092.
19. M. Y. Yen, M. C. Hsiao, S. H. Liao, P. I Liu, H. M. Tsai, C. C. M. Ma, N. W. Pu and M. D. Ger, *Carbon*, 49 (2011) 3597.
20. W. Hong, Y. Xu, G. Lu, C. Li and G. Shi, *Electrochemistry Communications*, 10 (2008) 1555.
21. L. Wan, S. Wang, X. Wang, B. Dong, Z. Xu, X. Zhang, B. Yang, S. Peng, J. Wang and C. Xu, *Solid State Sciences*, 13 (2011) 468.
22. G. Zhu, T. Xu, T. Lv, L. Pan, Q. Zhao and Z. Sun, *Journal of Electroanalytical Chemistry*, 650 (2011) 248.

23. R.R. Nair, P. Blake, A. N. Grigorenko, K. S. Novoselov, T. J. Booth, T. Stauber, N. M. R. Peres and A.K. Geim, *Science*, 320 (2008) 1308.
24. M. Y. Han, B. Ozyilmaz, Y. B. Zhang and P. Kim, *Phys. Rev. Lett.*, 98 (2007) 206805.
25. F. Croce, G. B. Appetechi, L. Persi and B. Scrosati, *Nature*, 394 (1998) 456.
26. T. Caykara, S. Demirci, M. S. Eroglu and O. Guven, *Polymer*, 46 (2005) 10750.
27. M. S. Akhtar, J. G. Park, H. C. Lee, S. K. Lee and O-B. Yang, *Electrochimica Acta*, 55 (2010) 2418.
28. J. E. Trancik, S. C. Barton and J. Hone, *Nano Lett.*, 8 (2008) 982.
29. J. F. Dobson, *Surf. Sci.* (2011) doi:10.1016/j.susc.2010.12.031.
30. S. E. Bourdo and T. Viswanathan, *Carbon*, 43 (2005) 2983.
31. Z. Ning, Q. Zhang, W. Wu, H. Pei, B. Liu and H. Tian, *J. Org. Chem.*, 73 **(**2008) 3791
32. Y. Kim, B. J. Yoo, R. Vittal, Y. Lee, N. G. Park and K. J. Kim, *Journal of Power Sources*, 175 (2008) 914.
33. G. W. Lee, D. Kim, M. J. Ko, K. Kim and N. G. Park, *Solar Energy*, 84 (2010) 418.
34. S. R. Kim, Md. K. Parvez and M. Chhowalla, *Chemical Physics Letters*, 483 (2009) 124.
35. J. Zhang, T. Hreid, X. Li, W. Guo, L. Wang, X. Shi, H. Su and Z. Yuan, *Electrochimica Acta*, 55 (2010) 3664.
36. J. Van de Lagemaat, N. G. Park and A. J. Frank, *J. Phys. Chem. B*, 104 (2000) 2044.
37. Q. Wang, J. Moser and M. Gratzel, *J. Phys. Chem. B*, 109 (2005) 14945.
38. V. Ganapathy, B. Karunagaran and S. W. Rhee, *J. Power Sources*, 195 (2010) 5138.
39. K. M. Lee, V. Suryanarayanan and K. C. Ho, *Sol. Energy Mater. Sol. Cells*, 91 (2007) 1416.